Rotational Resonance NMR Measurements of Internuclear Distances in an α-Helical Peptide

Olve B. Peersen,[†] Shoko Yoshimura,[‡] Hironobu Hojo,[‡] Saburo Aimoto,[‡] and Steven O. Smith*,[†]

Contribution from the Department of Molecular Biophysics and Biochemistry, Yale University, New Haven, Connecticut 06511, and the Institute for Protein Research, Osaka University, Osaka, Japan. *Received October 21, 1991*

Abstract: Magnetization transfer rates have been measured between specific ^{13}C sites of an α-helical undecapeptide in crystals and in membrane bilayers by rotational resonance NMR methods. A comparison of the rates of magnetization transfer for five peptides bearing pairs of ^{13}C labels separated by 3.7–6.8 Å with the internuclear distances obtained from the X-ray crystal structure of the peptide is used to define the resolution and limits of rotational resonance NMR for distance determinations. These studies demonstrate that $^{13}C\cdots{}^{13}C$ distances up to 6.8 Å can be measured with an accuracy of ~0.5 Å. Comparison of the NMR data from peptide crystals with that from peptides reconstituted into lipid bilayers shows that the peptide maintains a helical structure and that these measurements can be extended to membrane systems.

Introduction

There are few high-resolution structural studies of integral membrane proteins using well-established diffraction and solution NMR methods. It has generally been a challenge to grow well-ordered crystals of large hydrophobic proteins for diffraction studies, while solution NMR approaches rely on rapid isotropic molecular motion and encounter problems with the large line widths characteristic of protein–lipid complexes. Solid-state NMR approaches, in comparison, are well-suited for studying large heterogeneous systems with restricted motion and have been effective in structural studies of membrane proteins, such as gramicidins,[1,2] rhodopsins,[3] and phage coat proteins.[4,5] Recent advances in magic angle spinning (MAS) methods for measuring both homonuclear[6,7] and heteronuclear[8] distances extend the potential of solid-state NMR for obtaining high-resolution structural data in these systems. Previous rotational resonance (RR) NMR studies of zinc acetate[6] and tyrosine ethyl ester[9] have shown that this technique can be used to investigate $^{13}C\cdots{}^{13}C$ distances as long as 5 Å with a resolution, based on numerical simulations, of ~0.5 Å. In this study, we use a hydrophobic α-helical peptide to further characterize the resolution and limits of the rotational resonance NMR approach and to explore its utility in determining the local secondary structure of membrane-bound peptides in phospholipid bilayers.

The undecapeptide selected for the RR NMR studies has the sequence Boc-L-Ala-{Aib-Ala}$_2$-Glu(OBzl)-Ala-{Aib-Ala}$_2$-OMe and contains several helix-forming aminoisobutyric acid (Aib) residues. It has previously been used to model the N-terminus of alamethicin, a 20 amino acid peptide that forms voltage-gated pores in membrane bilayers.[10,11] The X-ray crystal structure of the undecapeptide has been solved and refined to 0.9-Å resolution by Jung and co-workers[12] and also as a part of this study. In both structures the first nine residues form an α-helix and the atomic coordinates are well-defined. Furthermore, the peptide is hydrophobic and can be reconstituted into lipid bilayers. Rotational resonance measurements on the undecapeptide extend the previous RR studies by providing a means of comparing magnetization transfer rates between several ^{13}C pairs that are chemically identical and differ only in their internuclear separations and molecular orientations. These measurements can be made both in crystals, where the ^{13}C distances and orientations are known from the X-ray structure, and in membranes. Five different ^{13}C-labeled peptides have been synthesized, each containing two specific labels with internuclear distances ranging from 3.7 to 6.8 Å. The ^{13}C labels have been placed on alanine methyl and backbone carbonyl carbons in the first five residues of the peptide. Several labels are separated by three to four residues in the amino acid sequence but lie close together in space because of the helical geometry of the peptide. Magnetization transfer rates between these sites report directly on the peptide secondary structure.

Theory

Rotational resonance NMR uses the rotational frequency of the sample in a MAS NMR experiment to selectively restore the dipolar coupling between two dilute nuclear spins, such as the ^{13}C labels in the experiments described below. This is achieved by spinning the sample at a rate ω_r such that $\Delta\omega = n\omega_r$, where n is a small integer and $\Delta\omega$ is the difference in the isotropic chemical shifts of the two ^{13}C resonances. In order to measure the dipolar coupling and thereby determine the distance between the two spins, one of the ^{13}C resonances is selectively inverted and the intensity of one or both of the resonances is monitored as a function of a mixing time during which nuclear spin magnetization is exchanged. When spinning at the $n = 1$ resonance condition, the initial rate of magnetization transfer is dominated by the dipolar coupling, which is proportional to the inverse cube of the internuclear distance. Levitt et al.[13] have presented a detailed discussion of RR phenomena and show in simulations that only minor contributions to the $n = 1$ transfer rate come from the relative geometry of the ^{13}C-labeled functional groups. Increasing the value of n decreases the rate of transfer and causes the dependence on molecular orientation to become more pronounced, making interpretation of the transfer rate more difficult. Simulations of strongly coupled sites predict line-shape effects and oscillations in the transfer rate due to the relative orientations of the chemical shift tensors of the exchanging nuclei, but in practice these are

[†] Yale University.
[‡] Osaka University.

(1) Nicholson, L. K.; Cross, T. A. *Biochemistry* **1989**, *28*, 9379–9385.
(2) Teng, Q.; Nicholson, L. K.; Cross, T. A. *J. Mol. Biol.* **1991**, *218*, 607–619.
(3) Smith, S. O.; Griffin, R. G. *Ann. Rev. Phys. Chem.* **1988**, *39*, 511–535.
(4) Opella, S. J.; Stewart, P. L.; Valentine, K. G. *Quart. Rev. Biophys.* **1987**, *19*, 7–49.
(5) Shon, K. J.; Kim, Y.; Colnago, L. A.; Opella, S. J. *Science* **1991**, *252*, 1303–1305.
(6) Raleigh, D. P.; Levitt, M. H.; Griffin, R. G. *Chem. Phys. Lett.* **1988**, *146*, 71–76.
(7) Colombo, M. G.; Meier, B. H.; Ernst, R. R. *Chem. Phys. Lett.* **1988**, *146*, 189–196.
(8) Gullion, T.; Schaefer, J. In *Advances in Magnetic Resonance, 13*; Warren, W. S., Ed.; Academic Press: New York, 1989; pp 57–83.
(9) Raleigh, D. P.; Creuzet, F.; Gupta, S. K. D.; Levitt, M. H.; Griffin, R. G. *J. Am. Chem. Soc.* **1989**, *111*, 4502–4503.
(10) Fox, R. O.; Richards, F. M. *Nature* **1982**, *300*, 325–330.
(11) Cascio, M.; Wallace, B. A. *Proteins* **1988**, *4*, 89–98.
(12) Bosch, R.; Jung, G.; Schmitt, H.; Winter, W. *Biopolymers* **1985**, *24*, 961–978.
(13) Levitt, M. H.; Raleigh, D. P.; Creuzet, F.; Griffin, R. G. *J. Chem. Phys.* **1990**, *92*, 6347–6364.

0002-7863/92/1514-4332$03.00/0

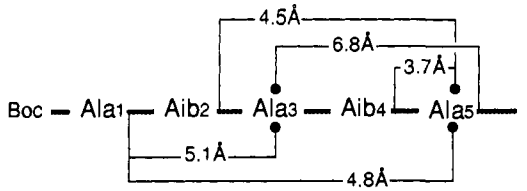

Figure 1. N-Terminal sequence of the undecapeptide showing the positions and distances between the ^{13}C-labeled pairs. The lines originate at backbone carbonyls and terminate with dots at alanine methyl groups.

generally not observed for $^{13}C\cdots^{13}C$ distances above 4 Å due to weak dipolar coupling and damping by zero quantum (ZQ) T_2 effects. Magnetization exchanges only very slowly when the sample is not spinning on rotational resonance, i.e., when n is not an integer.

The pulse sequence used for rotational resonance NMR consists of a standard solid-state cross-polarization sequence[14,15] immediately followed by a ^{13}C flip-back pulse and selective inversion of one of the two resonances being studied. The NMR signal is detected after a variable mixing time during which magnetization is allowed to exchange between the two sites. As mentioned above, if the two rotationally coupled spins are also close in space and coupled by a strong dipolar interaction, then transfer of magnetization between them will manifest itself as a modulation of the intensities of the resonances as a function of the mixing time. The data are analyzed as a magnetization transfer curve obtained by calculating the intensity difference between the two resonances as a function of mixing time and normalized to an initial intensity of 1.0.

Experimental Section

Five different ^{13}C-labeled peptides were synthesized according to the methods of Schmitt et al.[16] using *t*-Boc amino acid derivatives. The ^{13}C labeling scheme is illustrated in Figure 1. The crystals used for this study were grown by diluting ^{13}C-labeled peptide 1:10 with unlabeled peptide in a minimal volume of methanol and then allowing the solvent to evaporate, resulting in dry needlelike crystals, which were subsequently broken into microcrystals to provide a well-balanced sample for magic angle spinning. The ^{13}C-labeled peptide was diluted to produce well-isolated $^{13}C\cdots^{13}C$ spin pairs in the crystal lattice and reduce any intermolecular transfer in the RR experiments. The above crystallization conditions differ from those of Jung and co-workers, and as a result the X-ray structure of the crystals used for the NMR measurements was determined. The earlier crystallization conditions (solubilization in dichloromethane followed by addition of diethyl ether) produced crystals that were not stable in the absence of mother liquor.[12,16] The X-ray structure of the methanolic crystals was determined using a 0.03 × 0.25 × 0.20 mm crystal with $P2_1$ symmetry and unit cell dimensions of a = 12.261 (4) Å, b = 18.693 (3) Å, c = 13.591 (4) Å, β = 101.38 (2)°, Z = 2, and V = 3054 (1) Å^3. 3174 unique reflections with $I > 2\sigma$ were collected to a maximum 2θ value of 116.1° using Cu Kα radiation and a Rigaku AFC5S diffractometer. The structure was solved and refined (R = 0.090) using direct methods and the TEXSAN structure analysis package from Molecular Structure Corp. The major differences between the two crystal structures are in the positions of the two C-terminal amino acids and the O-benzyl group attached to the glutamic acid residue (Figure 2). The backbone atoms of the helix are virtually superimposable with an rms deviation of 0.11 Å for residues 1–9. The rms difference between the structures of the first five residues, where the ^{13}C labels are located, is 0.08 Å for all atoms and the largest difference for a single pair of $^{13}C\cdots^{13}C$ labels is 0.14 Å. All distances quoted are from the crystals grown from methanol solutions and used for the NMR experiments.

The reconstitution of peptide into lipid bilayers was accomplished by separately solubilizing the peptide and dipalmitoylphosphatidylcholine (DPPC) in 5% sodium dodecyl sulfate (SDS), combining the solutions at a 1:10 molar ratio, and then precipitating the SDS by adding potassium.[17] Residual SDS was removed by dialysis. Lipid vesicles containing peptide sedimented as a single band in sucrose density gradient centrifugation. The NMR experiments of the lipid preparations were conducted at −40 °C to reduce molecular motion and increase the signal intensity.

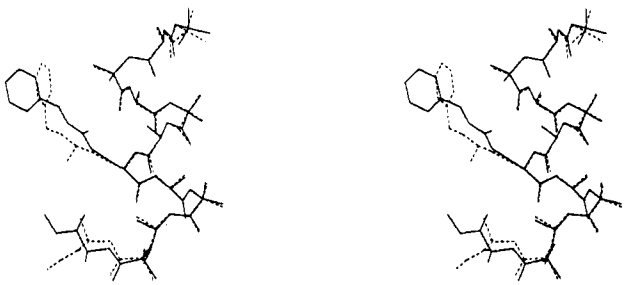

Figure 2. Two X-ray crystal structures of the alamethicin peptide oriented with the N-terminus at the top of the figure. The rms difference between the two structures is 0.11 Å for the backbone atoms of the α-helix (residues 1–9) and 0.08 Å for all atoms in residues 1–5. The solid line is the structure obtained by evaporation of methanol and the dotted line is the structure from dichloromethane by the addition of ether.[12]

The ^{13}C NMR spectra were collected at 50.3 MHz on a Bruker MSL-200 spectrometer with a home-built probe employing either a 5-mm high-speed or 7-mm standard magic angle spinner from Doty Scientific (Columbia, SC). The pulse sequence used was similar to that described previously,[6] but using a DANTE pulse train[18] for selective inversion rather than a long low power pulse. The proton power was adjusted for a 4-μs 90° pulse length with a cross-polarization (CP) pulse of 2.5 ms and an acquisition delay of 2.5 s. The spectral width was 25 kHz. All the spectra presented represent 1024 FIDs processed with 20 Hz line broadening and zero filled from 1K to 2K points with a final resolution of 12.2 Hz per point. The carbonyl resonance was inverted with a DANTE pulse train consisting of five to seven 1.2-μs pulses (at the carbonyl frequency) separated by 100 μs; the resulting frequency domain echoes are separated by 10 kHz and as a result do not affect other parts of the ~8-kHz-wide ^{13}C spectrum. The non-rotor-synchronized DANTE pulse train results in a ~20% intensity loss when compared to a normal CP spectrum taken at the same spinning speed ($\omega_r \cong 8$ kHz). In order to average out spectrometer instabilities the RR mixing times were randomly scrambled and the data were collected in interleaved blocks of 256 or 128 acquisitions. The precise rotational resonance spinning speed, ranging from 7922 to 8081 Hz, was determined independently for each of the five peptides and controlled to within ±5 Hz by using a home-built spinning speed controller.[19]

The RR transfer curves were calculated by integration of the carbonyl and alanine methyl peaks from all of the spectra in a given mixing time series. The initial intensity of each ^{13}C label was determined by averaging the short time (<2 ms) points, i.e., before RR transfer has taken place, and a natural abundance contribution was calculated as a percentage of this full intensity (see below). This natural abundance value was then subtracted from all time points in the series, the difference between the methyl and carbonyl intensities was calculated for each time, and the resulting curve was normalized to an initial value of 1.0, again by averaging of the first few points. The natural abundance contribution to each peak, which does not undergo significant RR transfer and should not be included in the curve normalization factor, was determined by a least-squares subtraction of two normal CP spectra, one of the diluted ^{13}C-labeled material and the other a natural abundance spectrum of the peptide. There are several advantages to this method; the subtraction at the inverted resonance is not affected by differences in the inversion efficiency of the two spectra, the accuracy is improved by using control spectra with high signal-to-noise ratios, and any line broadening due to spinning at rotational resonance is removed by subtracting off rotational resonance spectra (~9 kHz for these peptides). Note that while this method corrects for natural abundance intensity in the spectra, it does not make a correction for competing magnetization transfer to natural abundance carbons in the crystal. An analysis of carbon–carbon distances in the packed crystal lattice shows that each pair of labels experiences 16–20 competing pathways to natural abundance carbonyl or alanine methyl groups within 7 Å. The average distance between a ^{13}C label and a natural abundance ^{13}C is about 5.3 Å. The Aib methyl groups differ in chemical shift[16] and are not at rotational resonance. Only

(14) Pines, A.; Gibby, M. G.; Waugh, J. S. *J. Chem. Phys.* **1973**, *59*, 569–590.
(15) Schaefer, J.; Stejskal, E. O. *J. Am. Chem. Soc.* **1976**, *98*, 1031–1032.
(16) Schmitt, H.; Winter, W.; Bosch, R.; Jung, G. *Liebigs Ann. Chem.* **1982**, *1982*, 1304–1321.
(17) Popot, J. L.; Gerchman, S. E.; Engelman, D. M. *J. Mol. Biol.* **1987**, *198*, 655–676.
(18) Morris, G. A.; Freeman, R. *J. Magn. Reson.* **1978**, *29*, 433–462.
(19) de Groot, H. J. M.; Copié, V.; Smith, S. O.; Allen, P. J.; Winkel, C.; Lugtenburg, J.; Herzfeld, J.; Griffin, R. G. *J. Magn. Reson.* **1988**, *77*, 251–257.

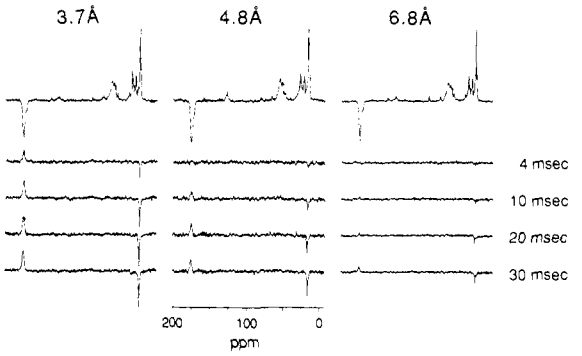

Figure 3. ^{13}C NMR transfer spectra of crystals of the undecapeptide at the $n = 1$ rotational resonance. The top spectrum corresponds to zero mixing time and the subsequent spectra are the differences obtained by subtraction of the zero time spectrum from those with mixing times of 4, 10, 20, and 30 ms. The line widths in the difference spectra of the 3.7-Å peptide are 140 and 75 Hz for the carbonyl and methyl resonances, respectively. Each spectrum corresponds to 1024 scans of ~10 mg of doubly ^{13}C-labeled peptide diluted with ~100 mg of unlabeled material.

one of the five peptides has a significant intermolecular pathway between the pair of labeled carbons; in this case the intermolecular distance is 5.09 Å, while the intramolecular distance is 5.12 Å. Accounting for 1.1% natural abundance ^{13}C and a 5.3-Å average distance, the competing natural abundance pathways are estimated to account for 8–10% transfer at 40 ms when $n = 1$, 2–3% of which is due to strong intraresidue (i.e., $Ala_n^{C=O}$ to $Ala_n^{CH_3}$ at 2.5 Å) and adjacent residue (i.e., $Aib_n^{C=O}$ to $Ala_{n+1}^{CH_3}$ at 3.7 Å) couplings.

Results and Discussion

The undecapeptide serves as a model system for characterizing local peptide structure by RR NMR. The Aib and Ala residues strongly favor a helical conformation[20,21] and the high-resolution crystal structures accurately define the atomic positions. RR measurements are described for a series of peptide crystals bearing pairs of ^{13}C labels with internuclear distances ranging from 3.7 to 6.8 Å that illustrate the range and resolution of the approach. The hydrophobic nature of the peptide favors its association with phospholipid bilayers and preliminary RR measurements on membrane-bound peptides are presented that show that this approach can be extended to membrane systems.

RR Measurements of Peptide Crystals. The spectra in Figure 3 illustrate magnetization transfer at the $n = 1$ rotational resonance for distances of 3.7, 4.8, and 6.8 Å in peptide crystals. In the top spectrum the ^{13}C-labeled carbonyl line (175 ppm) has been selectively inverted while spinning at rotational resonance with the ^{13}C-labeled methyl resonance (20 ppm). Exchange has not yet taken place in this zero mixing time spectrum. The subsequent spectra are difference spectra obtained by subtraction of this initial spectrum from those obtained by using longer mixing times, clearly illustrating an increase of the carbonyl signal coupled to a reduction of the methyl signal. Furthermore, the exchange is limited to the two rotationally coupled lines, with little or no transfer to the natural abundance α-carbons (50 ppm) or Aib methyl groups (25 ppm). The data have been summarized in Figure 4, which shows the normalized transfer curves for all five ^{13}C-labeled peptides at both the $n = 1$ and $n = 2$ rotational resonance conditions. The off-rotational resonance data corresponds to the 6.8-Å peptide spinning at 8500 Hz, which is 543 Hz faster than the $n = 1$ rotational resonance.

In the $n = 1$ transfer curves (Figure 4) the steepest slope and greatest magnetization transfer occurs between ^{13}C labels at $Aib_4^{C=O}$ and $Ala_5^{CH_3}$, which are only 3.7 Å apart in the crystal structure, and the transfer is rapid enough to just reveal the predicted oscillations in the transfer curve. The extent of damping of these oscillations, in conjunction with the known dipolar coupling from the X-ray distance, can provide an estimate of the T_2^{ZQ} in

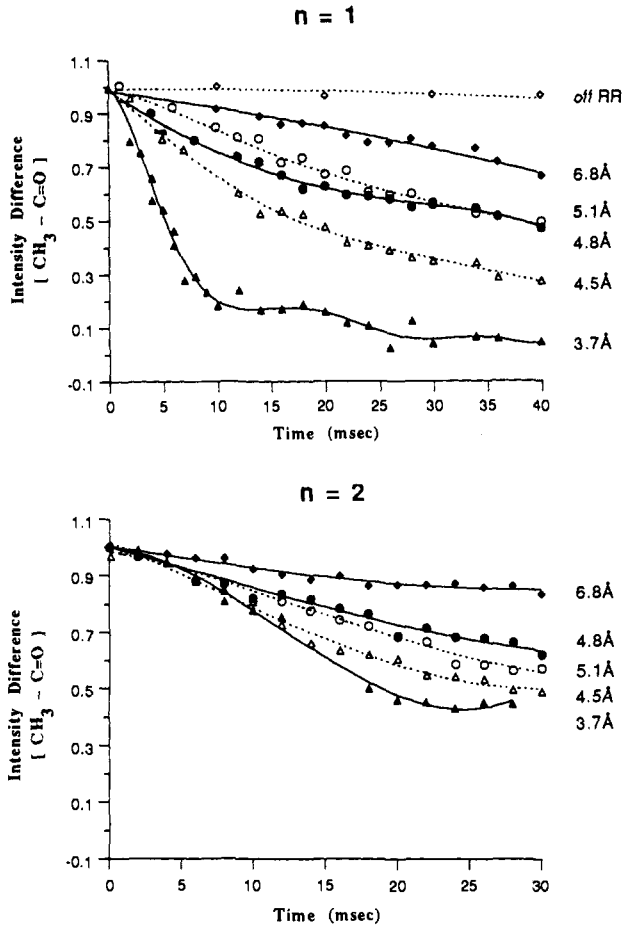

Figure 4. $n = 1$ and $n = 2$ $^{13}C\cdots{}^{13}C$ rotational resonance magnetization transfer curves for the five undecapeptides. The distances indicated are between backbone carbonyl and alanine methyl groups and correspond to $^{13}C\cdots{}^{13}C$ dipolar couplings of 151, 84, 68, 57, and 25 Hz. On the basis of the observed variation of peptide α-carbon intensities (50 ppm) during the rotational resonance experiments, the error in the normalized curves is 0.05 or less for all five peptides. The lines drawn are polynomial fits to illustrate the trend of the data; they are *not* theoretical simulations of transfer based on the molecular structure.

the peptide crystals. An accurate value of the T_2^{ZQ} is crucial when simulating data where oscillations are not present.[13] The next two curves are from ^{13}C pairs that directly test the secondary structure of the peptide via transfer between adjacent turns of the helix. Both pairs use one label at $Ala_5^{CH_3}$ with a second label at either $Ala_1^{C=O}$, yielding a 4.8-Å distance parallel to the helix axis, or at $Aib_2^{C=O}$, resulting in a 4.5-Å distance across the face of the helix. The helicity of the peptide is further explored by looking across the helix diameter, from $Ala_1^{C=O}$ to $Ala_3^{CH_3}$, where the crystal structure distance is 5.1 Å. The last peptide tests the limit of rotational resonance using $Ala_3^{CH_3}$ and $Ala_5^{C=O}$ labels, which are 6.8 Å apart in the crystal structure, the longest distance measured in these experiments. As shown in Figures 3 and 4, the transfer between these sites when $n = 1$ amounts to ~30% after 40 ms, and even with 10% transfer to natural abundance carbons the remaining 20% is easily resolved from the off-rotational resonance data. Taken together, the set of five transfer curves shown in Figure 4 illustrate the potential of the rotational resonance NMR approach for determining accurate distances in protein microcrystals and provide a set of standard curves that can be used for calibration of rotational resonance experiments between carbonyl and methyl groups. Importantly, these data show experimentally that the $n = 1$ transfer rates are dominated by the dipolar coupling and are not significantly influenced by the relative orientations of the methyl and carbonyl groups. The accuracy of the RR measurements clearly depends on the actual distance being measured because of the r^3 dependence of the dipolar coupling, as is easily seen by comparing the 3.7- and 4.5-Å

(20) Karle, I. L.; Balaram, P. *Biochemistry* **1990**, *29*, 6747–6756.
(21) Karle, I. L.; Flippen-Anderson, J. L.; Uma, K.; Balaram, P. *Proteins* **1990**, *7*, 62–73.

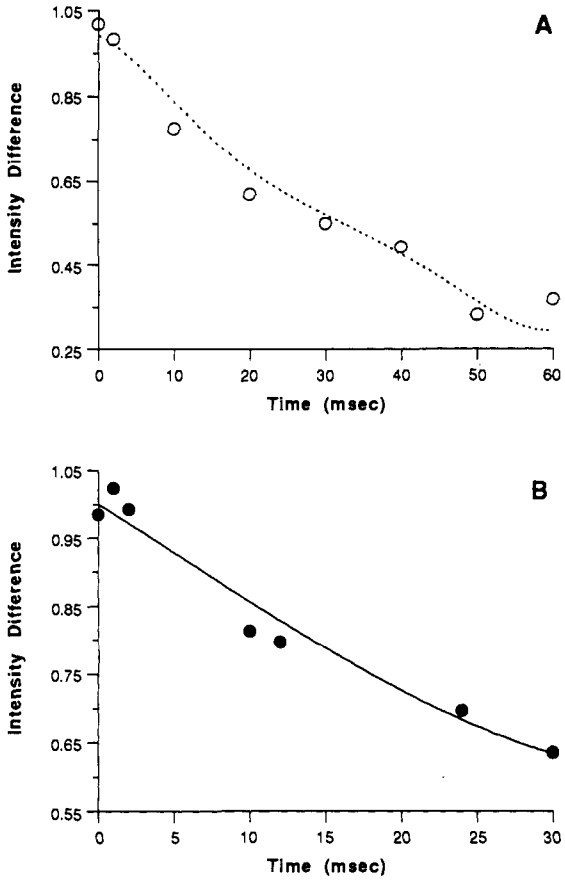

Figure 5. Transfer curves for peptide–DPPC complexes. Shown are the 5.1-Å peptide spinning at $n = 1$ (A) and the 4.8-Å peptide at $n = 2$ (B). The lines correspond to the crystal data for each peptide and the symbols are the data from DPPC-reconstituted peptides. The lipid data were collected at a temperature of −40 °C to reduce peptide motion.

curves (0.8-Å difference) and the 5.1- and 6.8-Å curves (1.7-Å difference). Even though the initial transfer rate at 4.8 Å is faster than that at 5.1 Å, the transfer curves eventually merge, implying that 0.3 Å is the approximate resolution limit of the method at distances in the vicinity of 5 Å.

When the magic angle spinning rate is decreased so that $n = 2$, i.e., $\omega_r = \sim 4$ kHz in these experiments, the transfer rates decrease (Figure 4), but there continues to be significant transfer. Experimentally this is quite important because the $n = 2$ experiments are generally more feasible, requiring slower spinning speeds and allowing larger sample volumes to be used. The most significant observation from the $n = 2$ data is the apparent reversal of the 4.8- and 5.1-Å transfer curves; in this case the ^{13}C labels separated by the longer distance appear to be exchanging more rapidly. As shown by the $n = 1$ data, the 0.3-Å difference between these distances appears to be the limit of resolution, raising the possibility that orientation effects play a significant role in the $n = 2$ data. This is currently being investigated with theoretical simulations of the transfer rates based on distances and orientations available from the crystal structure.

RR Measurements of Membrane-Bound Peptides. The structure of the peptide when bound to a membrane has been addressed by reconstituting ^{13}C-labeled peptides into lipid bilayers. RR measurements in membranes are complicated by the increased motion and structural flexibility of the peptide, since it is no longer held in a crystal lattice. As pointed out earlier, the presence of the conformationally restrictive Aib residues in the peptide favors a helical conformation, and potential problems with motion have been countered by lowering the sample temperature to −40 °C. Figure 5 shows a comparison of transfer rates in the crystals and in lipid for the 4.8- ($n = 2$) and 5.1-Å ($n = 1$) peptides, the two pairs most sensitive to changes in secondary structure. The close correlation of these two data sets with the crystal data provides the first indication that the RR NMR methods will work at low temperature for small peptides incorporated into membranes. Further experiments to explore the temperature dependence of magnetization transfer are in progress.

These results set the stage for extending the RR methods to membrane systems in order to study the local secondary structure and possibly tertiary fold of membrane proteins. Two challenges for larger systems involve specifically targeting ^{13}C pairs, possibly by using heteronuclear spectral editing approaches to target unique ^{15}N–^{13}C peptide bonds,[22-24] and accurate subtractions of protein background signals. The effective 10-kDa protein background in the crystal experiments discussed above (due to dilution with unlabeled material) and studies of ^{13}C-labeled retinal in the 26-kDa protein bacteriorhodopsin[25] illustrate that moderately large systems are tractable.

In conclusion, we show that the distance range of rotational resonance magnetization transfer is sufficient to investigate local peptide secondary structure, and when the experiment is performed at the $n = 1$ rotational resonance the interpretation of the initial transfer rate is straightforward. Furthermore, a set of control curves for the system, such as the carbonyl–methyl transfer curves presented in this paper, can be used to estimate distances up to 7 Å, and with the proper use of backbone ^{13}C labels this is sufficient to discriminate between α-helical and β-sheet structures.

Acknowledgment. We thank Gayle Schulte for the X-ray crystallography and Shy Arkin for assistance with lipid sample preparation. This work was supported by NIH (GM 41212) and the Searle Scholars Program/Chicago Community Trust.

Supplementary Material Available: Listing of crystallographic experimental details and X-ray coordinates with isotropic temperature factors (7 pages). Ordering information is given on any current masthead page.

(22) Schneider, D. M.; Tycko, R.; Opella, S. J. *J. Magn. Reson.* **1987**, *73*, 568–573.
(23) Oas, T. G.; Hartzell, C. J.; Drobny, G. P.; Dahlquist, F. W. *J. Magn. Reson.* **1989**, *81*, 395–399.
(24) Stejskal, E. O.; Schaefer, J.; McKay, R. A. *J. Magn. Reson.* **1984**, *57*, 471–485.
(25) Creuzet, F.; McDermott, A.; Gebhard, R.; van der Hoef, K.; Spijker-Assink, M. B.; Herzfeld, J.; Lugtenburg, J.; Levitt, M. H.; Griffin, R. G. *Science* **1991**, *251*, 783–786.